Tetons 4: Galactic Structure, Stars, & the Interstellar Medium
ASP Conference Series, Vol. 231, 2001
C. E. Woodward, M. D. Bicay, and J. M. Shull, eds.

Atomic Gas in Evolved Stars: PDRs or Shocks?

Margaret Meixner, David Fong, & Edmund C. Sutton

University of Illinois, Dept. of Astronomy, MC-221, Urbana, IL 61801 USA

Arancha Castro-Carrizo & Valentín Bujarrabal

Observatorio Astronómico Nacional, Apartado 1143, E-28800, Alcalá de Henares Spain

William B. Latter

Caltech, SIRTF Science Center, MS 314-6, Pasadena, CA 91125 USA

Alexander Tielens

Kapteyn Astronomical Inst. Postbus, 800, Groningen, 9700 Netherlands

Douglas M. Kelly

University of Arizona, Steward Obs., Tucson, AZ, 85721 USA

Michael J. Barlow

Department of Physics and Astronomy, University College London, Gower Street, London WC1E 6BT United Kingdom

Abstract. We present results from an Infrared Satellite Observatory (ISO) SWS and LWS study of low-excitation atomic gas in 24 evolved stars which span the evolutionary phases from the asymptotic giant branch star to the planetary nebula phase. These data are analyzed in the context of photodissociation regions and shocked-gas regions. We find that photodissociation, not shocks, is responsible for the chemical change from molecular to atomic gas in all these sources, except for AFGL 618. The low-excitation atomic gas masses are estimated from the [CII] 158 μm line.

1. Introduction

Evolved stars are objects which return most of the matter to the interstellar medium, thereby enriching the Galaxy with heavier elements. They are also ideal astrophysical laboratories in which to study physical processes occurring in the Galaxy on a larger scale, such as photodissociation regions (PDRs) and shocked gas regions. Here we investigate the relative importance of photodissociation and shocks in the chemical evolution of planetary nebulae. Fong et al. (2000)

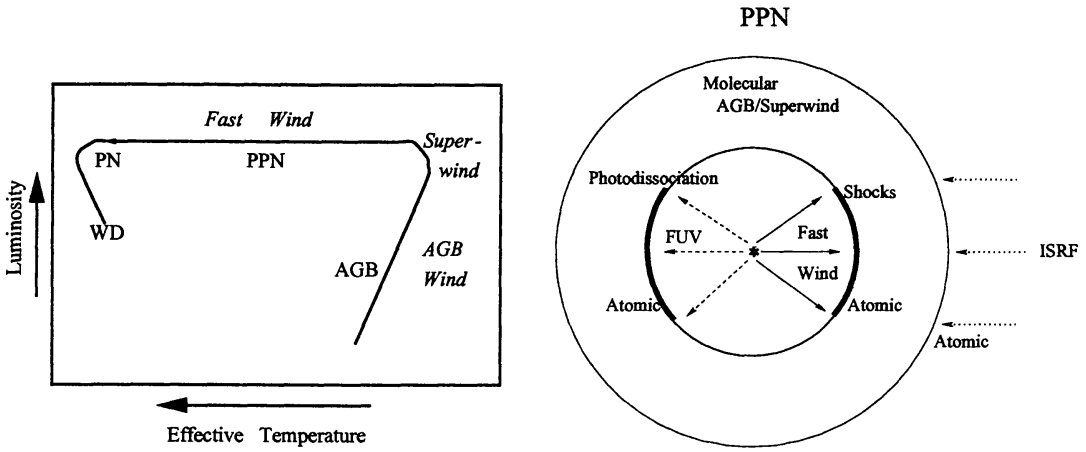

Figure 1. *Left:* A schematic HR diagram illustrating the evolution of an AGB star into a PN. *Right:* A cartoon PPN circumstellar shell.

and Castro-Carrizo et al. (2000) describe more completely the results for the carbon-rich (C-rich) and oxygen-rich (O-rich) sources, respectively.

2. The Formation and Evolution of Planetary Nebulae

Intermediate mass stars (0.8 – 8.0 $M_\odot$) such as the Sun lose much of their mass during the late stages of stellar evolution (i.e., on the AGB), leaving a central stellar core with a mass of about 0.6 $M_\odot$ surrounded by an extensive envelope (e.g., Iben 1995). The evolution of the star is schematically summarized in Figure 1. The AGB phase lasts $\sim 10^5$ yr and is followed by the proto-planetary nebula (PPN) phase, which is a quick ($\sim 10^3$ yr) transition phase. When the object becomes ionized, it appears in the visible as a planetary nebula (PN) for $\sim 10^4$ yr and as the envelope disperses into the interstellar medium, the central star becomes a white dwarf (WD). Observational evidence suggests that three winds are involved in stripping the outer envelope off the star. The heavy mass loss on the AGB begins as a gentle breeze losing $10^{-8} - 10^{-6}$ $M_\odot$ yr^{-1} (AGB wind) with velocities of $\sim$10 km s^{-1} and increases to much higher rates of $10^{-5} - 10^{-3}$ $M_\odot$ yr^{-1} (superwind) at the end of the star's life on the AGB. As the circumstellar shell, which is created by the AGB and superwinds, coasts off the star, a fast wind ($< 10^{-8}$ $M_\odot$ yr^{-1}, 1000 km s^{-1}) develops at some point during the PPN phase and plows into the slower moving circumstellar shell, creating shocked gas regions, in which molecular species are dissociated and heated. Meanwhile, the radiation field incident on the circumstellar shell hardens as the stellar temperature increases from 2×10^3 K on the AGB to almost 2×10^5 K as a PN central star. Over a few thousand years, the initially molecular circumstellar shell is photodissociated, ionized, and heated, creating a nebula which glows in the optical and infrared. The interstellar radiation field (ISRF) will also photodissociate the circumstellar shell from the outside, an effect observed in AGB stars.

Given this formation scenario, a PPN circumstellar shell will be mainly molecular with the outer envelope photodissociated by the ISRF, the inner envelope photodissociated by the central star and the inner envelope shocked by

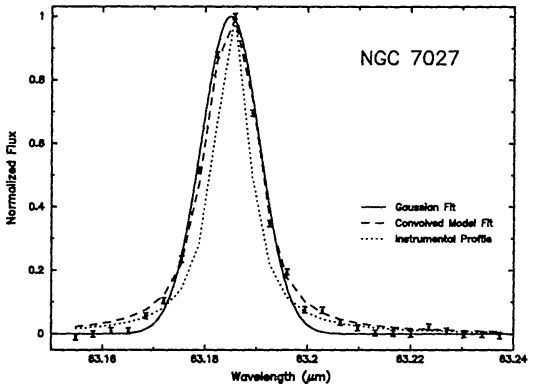

Figure 2. The [OI] 63 μm line from the C-rich PN, NGC 7027. The data points are compared with the instrumental profile (dotted line), a convolved model fit (dashed) and a Gaussian profile fit (solid). The Gaussian fit does not adequately account for the line wings. From Fong et al. (2000).

the fast wind (Fig. 1). A PN circumstellar shell will be similar to a PPN except that an H II region will be located between the PDR and the central star. Both the PDR and the shocked-gas region will have warm, low-excitation, atomic gas. However, the velocity of atomic gas in shocked regions will be higher than the expansion velocity of the molecular circumstellar shell while the atomic and molecular gas velocities will be comparable in the case of PDRs.

The relative role of the stellar radiation field and the stellar outflows in transforming the molecular ejecta into atomic gas is presently unknown. Infrared observations are a powerful probe of the warm atomic and molecular gas in PDRs and shocks (e.g., Hollenbach & Tielens 1997; Hollenbach & McKee 1989). Our ISO spectroscopy study of 24 evolved stars, presented here, addresses this issue.

3. ISO Observations

Using the ISO SWS and LWS, we observed far-infrared (FIR) atomic fine structure lines in a sample of 24 evolved stars which span the AGB, PPN and PN phases of evolution and which include an equal number of C-rich and O-rich objects. The far-infrared lines include: [NeII] 12.8 μm , [FeI] 24 and 35 μm , [SI] 25 μm , [FeII] 26 and 35 μm , [SiII] 35 μm , [OI] 63 and 146 μm , [SiI] 68 and 130 μm , [NII] 122 μm and [CII] 158 μm . Both grating and Fabry-Perot (FP) modes were used, however, only the lines observed with the FP are spectrally resolved. These data were reduced using standard routines. We developed line fitting routines for the FP data in Mathematica because the Gaussian fits of the standard routines were inadequate (Fig. 2). This code deconvolves the lines and estimates their width.

4. HR Diagram

Figure 3 plots the location of our entire sample on the HR diagram. The filled symbols indicate a detection of at least one of the far-infared lines (FIR). The

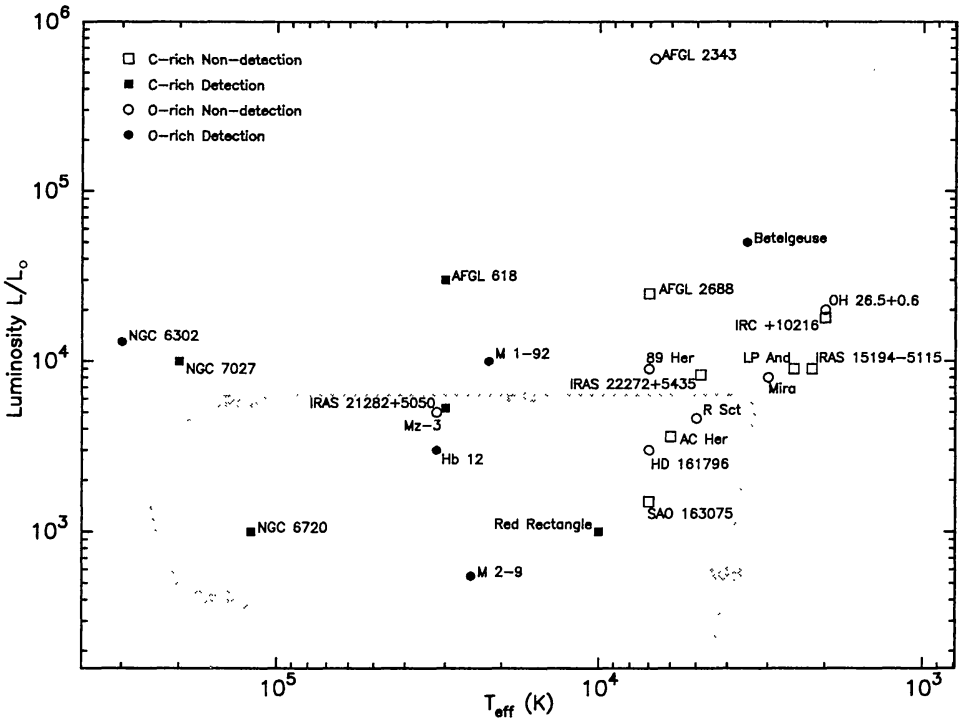

Figure 3. Objects from this ISO study plotted on the HR diagram. The name of the object appears near the symbol, defined in the legend. The dashed line is an evolutionary track for a star that will become a 0.6 $M_\odot$ WD. From Fong et al. (2000) and Castro-Carrizo et al. (2000).

Red Rectangle, which has an effective temperature of $\sim 10^4$ K, defines the lowest T_{eff} for detection in our sample and it is only detected in the [OI] 63 μm line. While Betelgeuse (a.k.a. α Ori) is also detected, it does not really belong in this sample because it is an M supergiant with an active chromosphere. As T_{eff} increases above the 10^4 K limit, the number of detected FIR lines increases and the intensity of these FIR lines increases. This general trend with T_{eff} is consistent with photodissociation by the central star being the main agent of chemical evolution from molecular to atomic gas.

5. Kinematics

The kinematics revealed by the FP lines also support the interpretation that these FIR lines arise in PDRs. For example, our model for the [OI] 63 μm line in NGC 7027 suggests a half width half maximum (HWHM) velocity of 23 ± 1 km s^{-1} (Fig. 2). The molecular envelope, which surrounds the PDR, is expanding at 20 km s^{-1} and the ionized gas, which is surrounded by the PDR, is expanding at 27 km s^{-1} as measured by our [NeII] 12.8 μm line. Thus the low-excitation atomic gas, traced by the [OI] line, appears to be expanding away from the central star at a similar rate as the molecular and ionized gas, as one would expect in a PDR. From this type of kinematic analysis, we find that in almost all of our sources, the FIR lines arise in PDRs, except for AFGL 618 and M2-9.

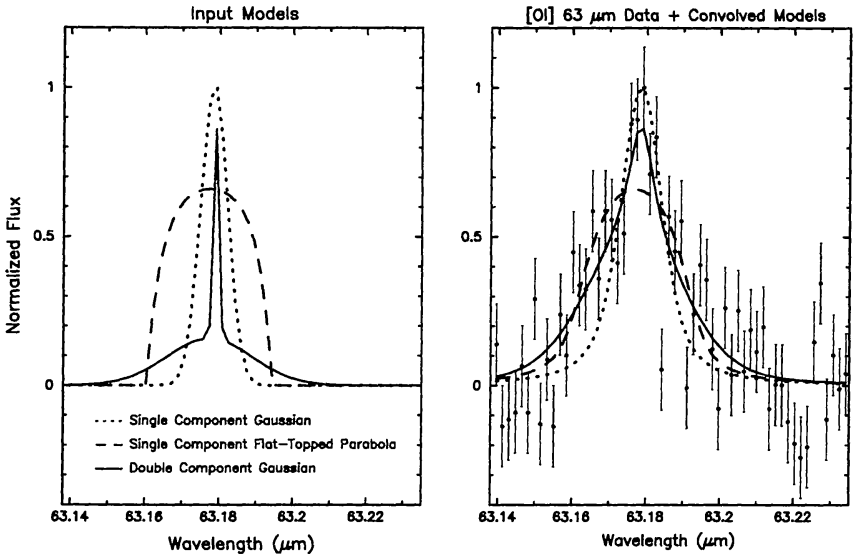

Figure 4. The [OI] 63 μm line from the C-rich PPN, AFGL 618. The model profile inputs (*left*) and the convolved models compared with the data. From Fong et al. (2000).

In the case of AFGL 618, a C-rich PPN, the best-fit profile has two components (Fig. 4): 1) a "PDR" component expanding at $\sim$ 20 km s^{-1} comparable to the bulk of the molecular gas (CO; e.g., Meixner et al. 1998) and to the ionized gas as measured by [NeII] 12.8 μm and 2) a "shocked-gas" component expanding at higher velocities of 66 km s^{-1}. While faster molecular gas is also observed in CO (e.g., Gammie et al. 1989), it is a very minor component and is probably related to this shocked-gas region. A PDR and shocked-gas component is also evident in the H_2 spectrum for AFGL 618 (e.g., Hora, Latter, & Deutsch 1998).

6. PDR and Shock Models

Comparison of the FIR line intensities with PDR and shocked-gas models also supports the interpretation that PDRs dominate the chemical evolution. Here we show the results for the C-rich evolved stars because the PDR models differ for a C-rich vs. O-rich environment. Figure 5 compares the observed line intensities with the C-rich PDR models of Latter & Tielens (2000). The far-UV radiation incident on the circumstellar shell, G, is calculated from stellar parameters of the central star and the size of the nebula. The observed line intensities fall within the parameter space of the PDR models suggesting a good agreement. Gas densities have been derived from this comparison. Comparison of the FIR line intensities is considerably worse with shocked-gas models. Both J-shocks and C-shocks were considered. The comparison with the J-shock model for the [CII] 158 μm line is shown in Fig. 6. The production of [CII] 158 μm line emission is expected to be small in shocks because the column of gas is small. The fact that our source detections lie well above the curves suggest that the observed [CII] lines cannot be produced in shocks.

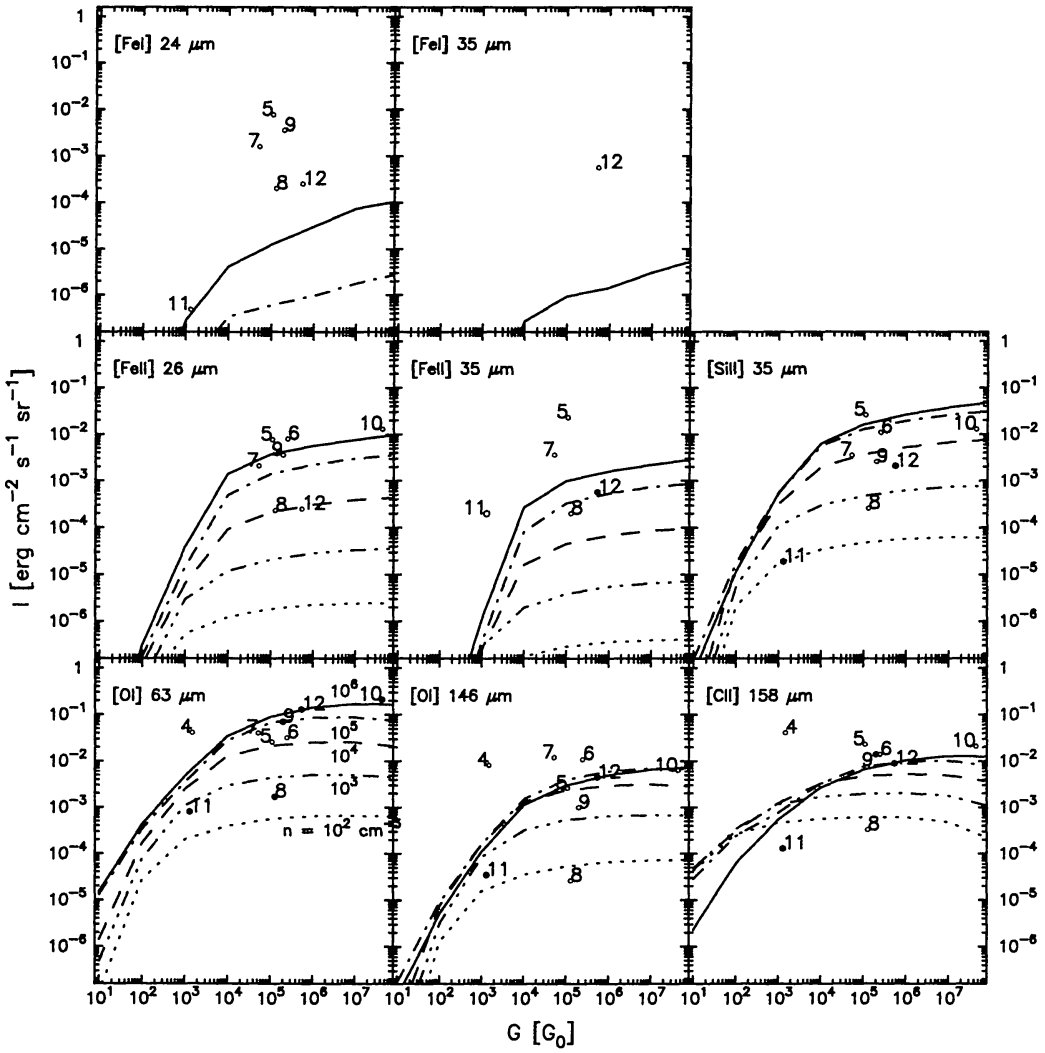

Figure 5. Comparison of the observed fine-structure atomic lines with the PDR model. The curves represent the predicted intensities for models with densities from 10^2 to 10^6 cm^{-3}. G is a measure of the incident far-UV radiation field in units of the ISRF (G_0). The filled circles indicate detections and the open circles indicate upper limits along the y-axis. The numeric symbols represent: 4–IRAS 22272+5435, 5–AC Her, 6–AFGL 2688, 7–SAO 163075, 8–Red Rectangle, 9–IRAS 21282+5050, 10–AFGL 618, 11–NGC 6720 and 12–NGC 7027. From Fong et al. (2000).

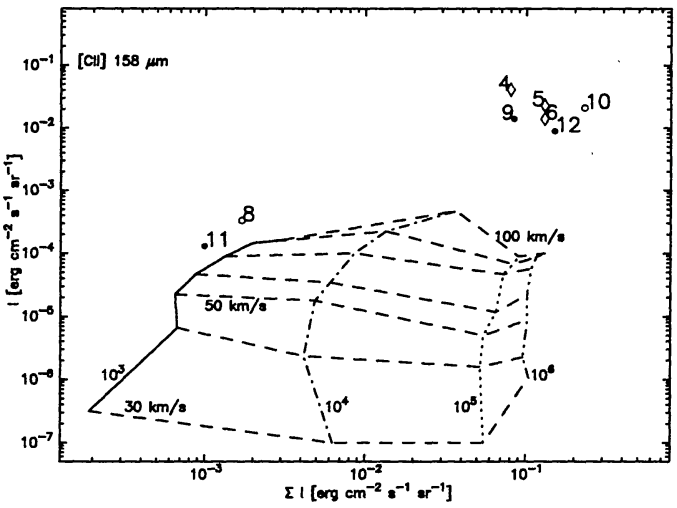

Figure 6. Comparison of the observed [CII] 158 μm line with the J-shock models of van den Ancker (1999). The curves represent the predicted intensities for models with densities from 10^3 to 10^6 cm^{-3} and velocities of 30 – 100 km s^{-1}. Symbols are the same as Fig. 5 with the addition that open diamonds indicate upper limits in both axes. From Fong et al. (2000).

7. Low-excitation Atomic Gas Masses

The mass of the low-excitation atomic gas in PDRs can be estimated from the [CII] 158 μm line intensity using the following formula,

$$\mathrm{M_{atomic}(M_\odot)} = 6.3\,10^6 \mathrm{F_{CII}(erg\,cm^{-2}\,s^{-1})\,D(kpc)^2\,F_c/X_C}\ , \qquad (1)$$

where $F_{\rm CII}$ is the observed [CII] flux, D is the distance, F_c is the correction factor when [CII] is not thermalized and $X_{\rm C}$ is the carbon abundance (Castro-Carrizo et al. 2000). In Table 1, we list the mass estimates for selected sources and their ionized and molecular masses, culled from the literature, for comparison. The sources are separated by chemistry and listed in order of increasing $T_{\rm eff}$. The low-excitation atomic gas mass increases as a star evolves from the PPN to PN phase as one would expect if photodissociation were the main agent of chemical evolution.

8. Conclusions

During the formation of a PN, photodissociation dominates the chemical evolution of the initially molecular circumstellar shell to low-excitation atomic gas. AFGL 618, a C-rich PPN, is exceptional in that it appears to have both a PDR and a shocked-gas contribution to its FIR atomic fine structure lines. The mass of low-excitation atomic gas, which we estimate from the [CII] 158 μm line, appears to increase with increasing $T_{\rm eff}$ of the central star.

Table 1. Low-Excitation Atomic Gas Masses

Source	$M_{ionized}$	M_{atomic}	$M_{molecular}$
C-rich			
IRAS 22272+5435	–	< 0.01	0.56
AC Her	–	< 0.01	$1.1\ 10^{-4}$
AFGL 2688	–	< 0.02	0.6
Red Rectangle	–	< 0.002	$2.5\ 10^{-5}$
IRAS 21282+5050	0.008	0.3	2.7
AFGL 618	$4\ 10^{-4}$	0.01*	1.6
NGC 6720	0.2	0.2**	0.34
NGC 7027	0.04	0.2	1.4
O-rich			
AFGL 2343	–	< 2	4.8
HD 161796	–	< 0.05	0.68
M 1-92	–	< 0.2	0.9
M 2-9	0.004	< 0.03	0.005
Hb 12	0.015	0.6	< 0.001
NGC 6302	0.2	1.5	0.1

*Questionable detection.
**Mass of the observed portion of NGC 6720 ($\sim 1/3$ of source).

References

Castro-Carrizo, A., Bujarrabal, V., Fong, D., Meixner, M., Tielens, A.G.G.M., Latter, W.B., & Barlow, M.J. 2000, A&A, submitted

Fong, D., Meixner, M., Castro-Carrizo, A., Bujarrabal, V., Latter, W.B., Tielens, A.G.G.M., Kelly, D.M., & Sutton, E.C. 2000, A&A, submitted

Gammie C.F., Knapp G.R., Young K., Phillips T.G., & Falgarone E., 1989 ApJ, 345, 87

Hollenbach D.& McKee C.F. 1989, ApJ, 342, 306

Hollenbach D.J. & Tielens A.G.G.M. 1997, ARA&A35, 179

Hora J.L., Latter W.B., & Deutsch L.K. 1999, ApJS, 124, 195

Iben, I. 1995, PhR, 250, 2

Latter, W.B. & Tielens, A.G.G.M. 2000, in preparation

Meixner M., Campbell M.T., Welch W.J., & Likkel, L. 1998, ApJ, 509, 392

van den Ancker, M. 1999, PhD Thesis, University of Amsterdam.